Supporting Information

Discrimination of Supramolecular Chirality using a Protein Nanopore

James A. Cooper, Stefan Borsley, Paul J. Lusby, and Scott L. Cockroft*

EaStCHEM School of Chemistry, University of Edinburgh, Joseph Black Building, David Brewster Road, Edinburgh EH9 3FJ, U.K

Contents

1. Synthesis and characterization

General

^{1}H and ^{13}C NMR spectra were recorded on a 500 MHz Bruker Avance III spectrometer, at a constant temperature of 25 °C, and processed using MestReNova 11.0. All peaks are reported in parts per million (ppm) from low to high field and referenced to the literature values for chemical shifts of residual non-deuterated solvent, with respect to tetramethylsilane. Circular dichroism spectra were recorded on a JASCO J-810 spectrapolarimeter. *N*-methylnicotinium iodide[1] and diastereopure, enantiopure[2] and racemic[3] coordination cages were synthesized as previously reported. Ion exchange to replace *S*-nic^{+} countercations with NMe_4^{+} counter-cations was carried out as previously reported[2] and confirmed by the absence of *S*-nic^{+} signals in ^{1}H NMR spectra.

Coordination Cages

^{1}H and ^{13}C NMR spectra obtained for all coordination cages were consistent with previously reported data.[2,#86] Circular dichroism spectra were obtained for the diastereomeric *N*-methylnicotinium salts of coordination cages and were in agreement with previously reported data.

Racemic-(K^{+}/NMe_4^{+})$_{11}$[$Ga_4L_6^{12-}$⊃ NMe_4^{+}]: ^{1}H NMR (500 MHz, D_2O) δ: Host: 7.93 (d, J = 7.5 Hz, 12H), 7.90 (d, J = 8.5 Hz, 12H), 7.32 (d, J = 8.5 Hz, 12H), 7.16 (t, J = 8.0 Hz, 12H), 6.80 (d, J = 7.0 Hz, 12H), 6.64 (t, J = 7.5 Hz, 12H); NMe_4^{+} (exterior): 2.67 (br s, 72 H) ; NMe_4^{+} (interior): Not observed following baseline correction; ^{13}C NMR (126 MHz, D_2O) δ: Host: 169.5, 158.0, 154.4, 133.7, 126.5, 126.3, 118.8, 117.4, 115.7, 115.1, 114.8, 114.7; Guest (NMe_4^{+}): 54.7.

ΛΛΛΛ-(K^{+}/*S*-nic^{+})$_{11}$[$Ga_4L_6^{12-}$⊃ *S*-nic^{+}]: ^{1}H NMR (500 MHz, D_2O) δ: Host: 7.86 (d, J = 7.7 Hz, 12H), 7.63 (d, J = 8.5 Hz, 12H), 7.33 (d, J = 8.3 Hz, 12H), 6.93 (t, J = 8.0 Hz, 12H), 6.81 (d, J =8.6 Hz, 12H), 6.64 (t, J = 7.7 Hz, 12H); *S*-nic^{+} (exterior): 7.67 (s, 5H), 7.59 (d, J = 7.3 Hz, 5H), 7.44 (br s, 5H), 7.06 (br s, 5H), 3.62 (s, 15H), 2.97 (br m, 5H), 2.70 (t, J = 7.6 Hz, 5H), 2.20 (q, J = 8.6 Hz, 5H), 1.82 (s, 15H), 1.74 (br m, 10H), 1.39 (br m, 5H); *S*-nic^{+} (interior): 8.00 (t, J = 7.0 Hz, 1H), 6.76 (d, 6.0 Hz, 1H), 5.14 (d, J = 8.5 Hz, 1H), 1.91 (s, 3H), −0.22 to −0.31 (m, 2 × signals, 1H and 3H), −0.63 (br m, 1H), −0.90 (br m, 1H), −1.13 (br m, 1H), −1.26 (br m, 1H), −1.52 (br m, 1H), −1.71 (br m, 1H); ^{13}C NMR (126 MHz, D_2O) δ: Host: 169.4, 158.5, 154.9, 133.4, 126.1, 118.5, 117.4, 115.2, 115.0, 114.8, 114.5; (*S*)-nic^{+} (exterior): 143.0, 142.9, 142.5, 141.5, 127.1, 66.4, 56.2, 47.7, 38.8, 32.5, 22.0; (*S*)-nic^{+} (interior): 144.6, 141.4, 137.8, 130.0, 64.1, 52.6, 45.6, 37.4, 32.9, 20.0.

ΔΔΔΔ-(K^{+}/*S*-nic^{+})$_{11}$[$Ga_4L_6^{12-}$⊃ *S*-nic^{+}]: ^{1}H NMR (600 MHz, D_2O) δ: Host: 7.88 (d, J = 7.7 Hz, 12H), 7.58 (d, J = 8.6 Hz, 12H), 7.33 (d, J = 8.3 Hz, 12H), 6.91 (t, J = 8.2 Hz, 12H), 6.81 (d, J = 7.3 Hz, 12H),

6.65 (t, J = 8.0 Hz, 12H); (*S*)-nic$^+$ (exterior): 7.87 (br s, 7H), 7.77 and 7.66 (2 × br s, 2 × 7H), 7.18 (br s, 7H), 3.78 (br s, 21H), 2.98 (br s, 7H), 2.91 (br s, 7H), 2.24 (br s, 7H), 2.03 (br s, 7H), 1.90 (s, 21H), 1.76 and 1.70 (2 × br s, 2 × 7H), 1.34 (br s, 7H); *S*-nic$^+$ (interior): 7.45 (t, J = 7.7 Hz, 1H), 6.28 (d, J = 5.6 Hz, 1H), 5.33 (d, J = 8 Hz, 1H), 4.24 (s, 1H), 1.90 (s, 3H), -0.03 (br m, 1H), 0.37 (t, J = 7.6 Hz, 1H), −0.67 (s, 1H), -0.88 (m, 2H), −1.05 (s, 3H), −1.23 (br m, 1H), −1.86 (br m, 1H); ^{13}C NMR (200 MHz, D_2O) δ: Host: 169.4, 158.6, 155.1, 133.4, 126.1, 125.9, 118.4, 117.2, 115.2, 114.8, 114.5; *S*-nic$^+$ (exterior): 143.0, 142.6, 142.2, 142.1, 127.1, 66.5, 56.2, 47.6, 39.0, 33.0, 22.0. *S*-nic$^+$ (interior): 144.6, 140.8, 140.3, 137.6, 127.0, 63.5, 53.1, 45.5, 36.3, 32.5, 20.9.

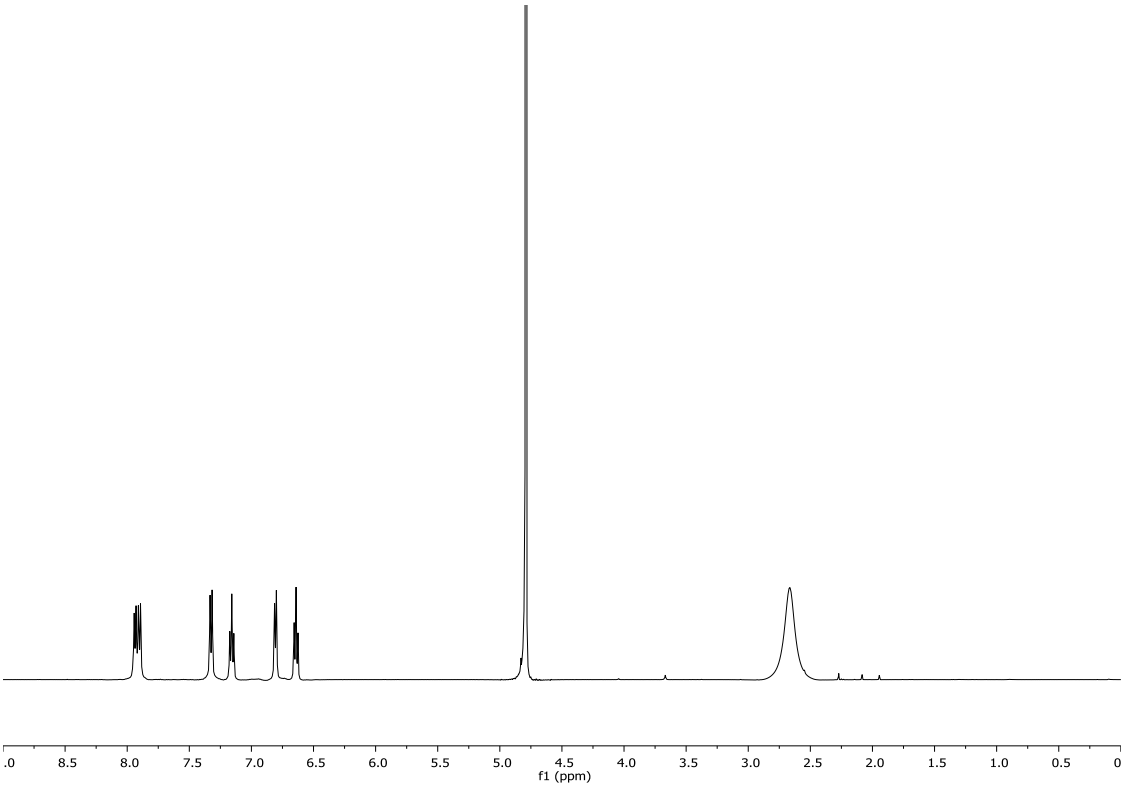

Figure S1. ^{1}H NMR (500 MHz, D_2O) of racemic $(K^+/NMe_4^+)_{11}[Ga_4L_6^{12-}\supset NMe_4^+]$.

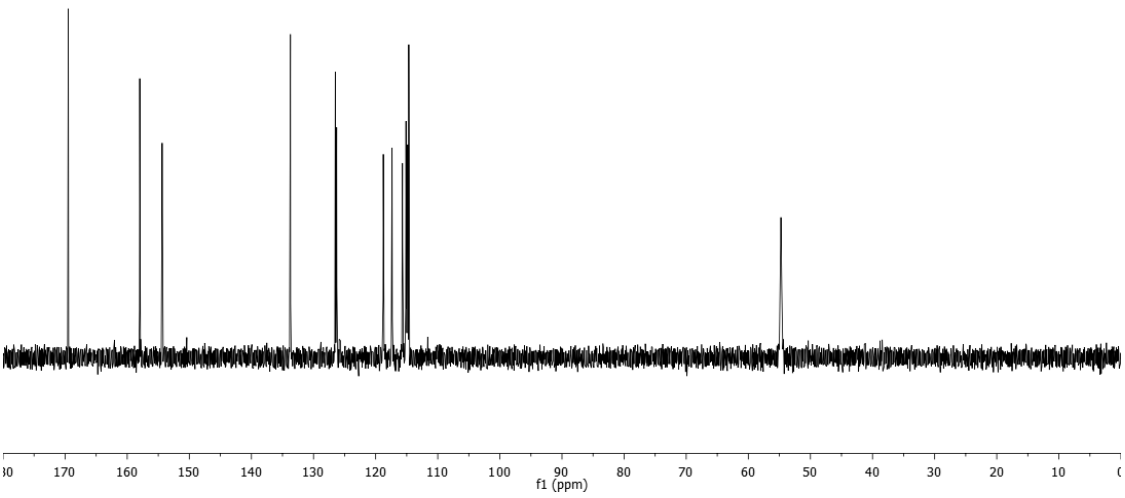

Figure S2. ^{13}C NMR (126 MHz, D_2O) spectrum of racemic $(K^+/NMe_4^+)_{11}[Ga_4L_6^{12-}\supset NMe_4^+]$.

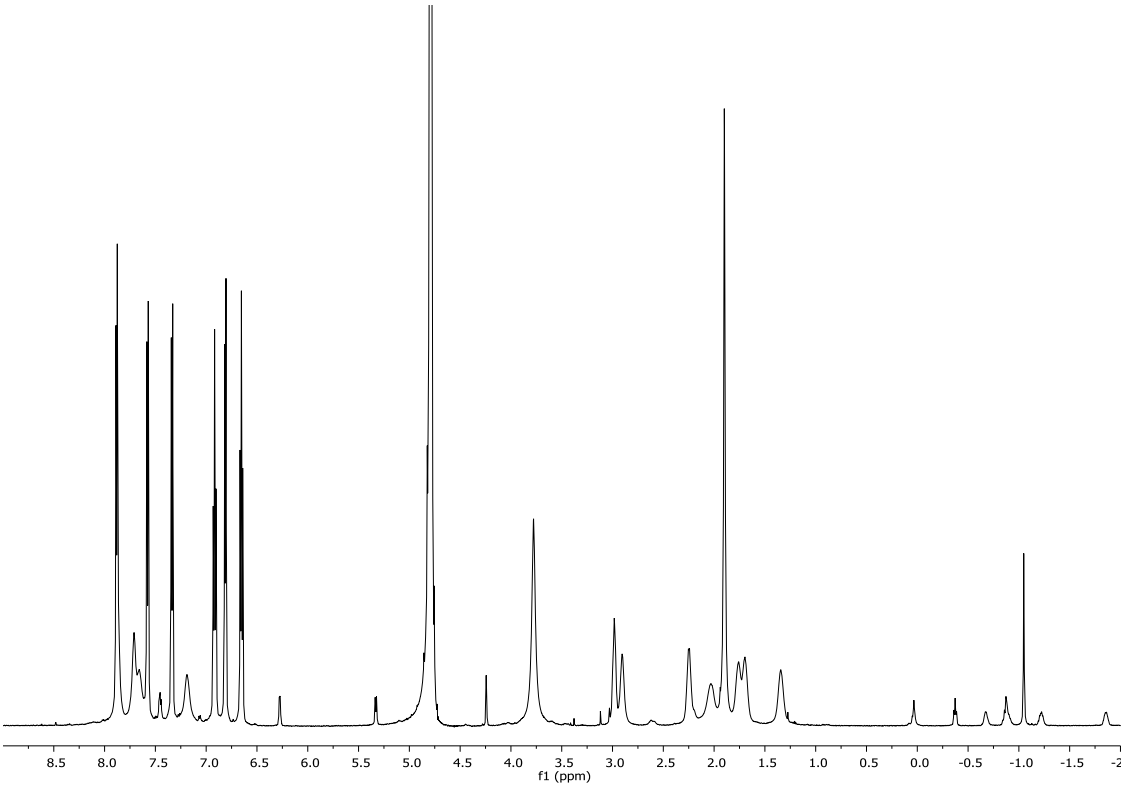

Figure S3. ^{1}H NMR (500 MHz, D_2O) of ΔΔΔΔ-(K^+/*S*-nic^+)$_{11}$[$Ga_4L_6^{12-}$⊃ *S*-nic^+].

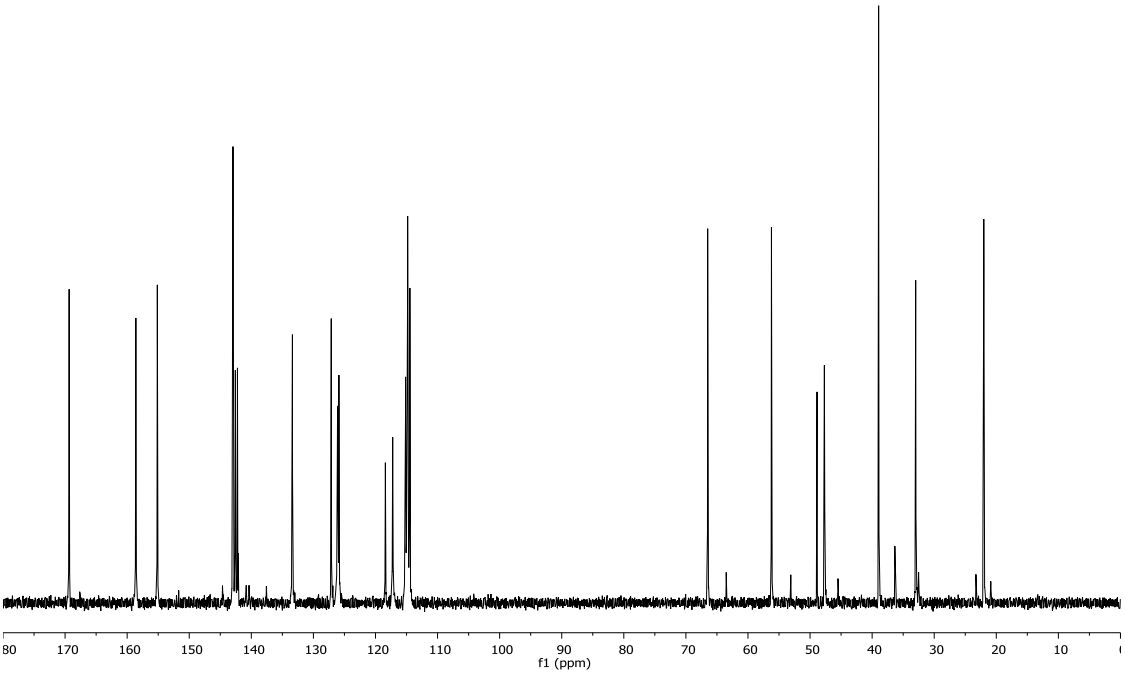

Figure S4. ^{13}C NMR (126 MHz, D_2O) spectrum of ΔΔΔΔ-(K^+/*S*-nic^+)$_{11}$[$Ga_4L_6^{12-}$⊃ *S*-nic^+].

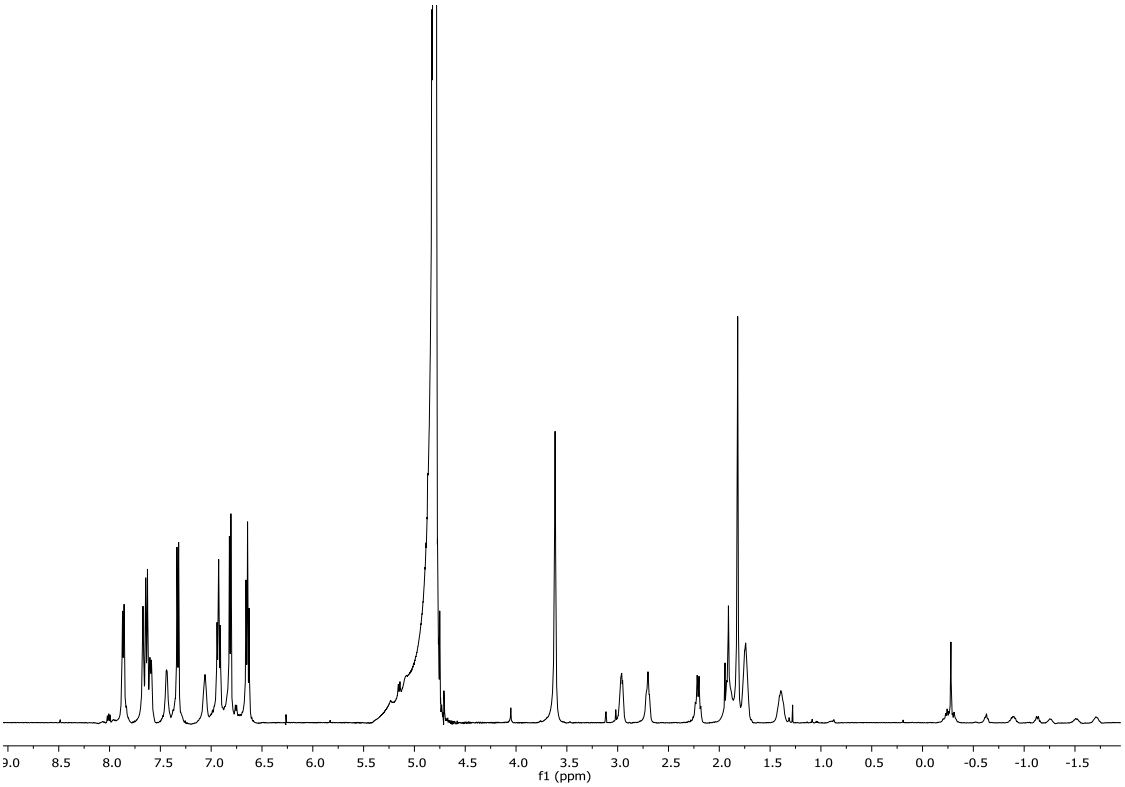

Figure S5. ^{1}H NMR (500 MHz, D_2O) spectrum of ΛΛΛΛ-(K^+/*S*-nic$^+$)$_{11}$[$Ga_4L_6^{12-}$⊃ *S*-nic$^+$].

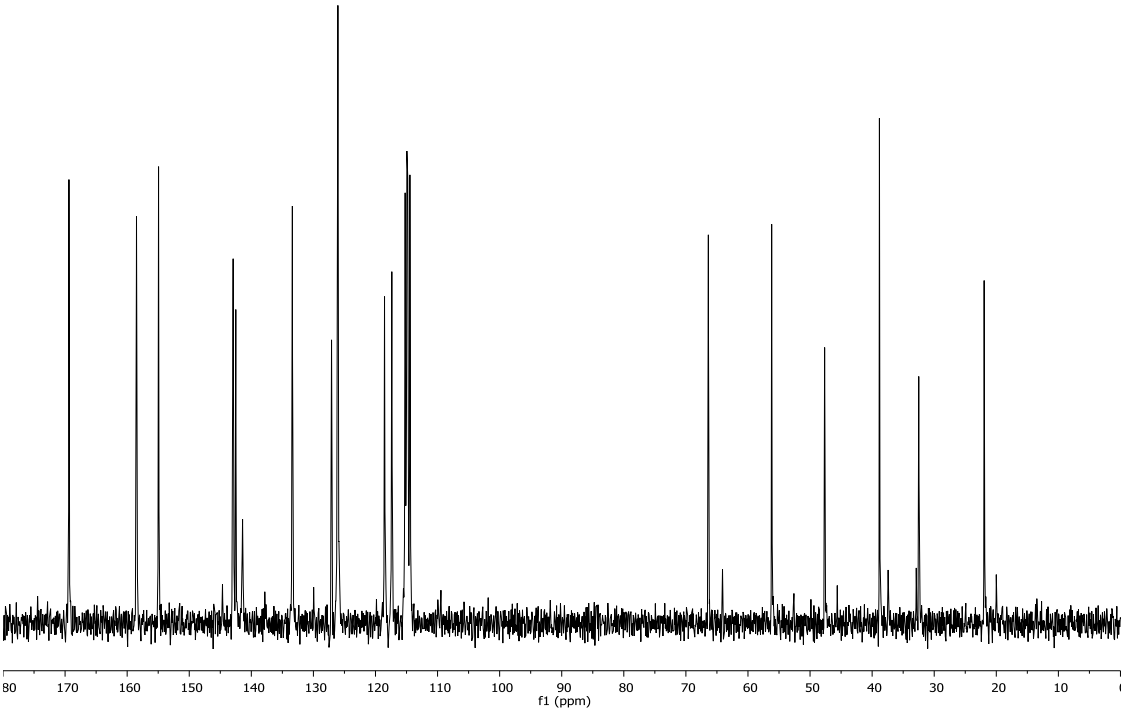

Figure S6. ^{13}C (126 MHz, D_2O) NMR spectrum of ΛΛΛΛ-(K^+/*S*-nic$^+$)$_{11}$[$Ga_4L_6^{12-}$⊃ *S*-nic$^+$].

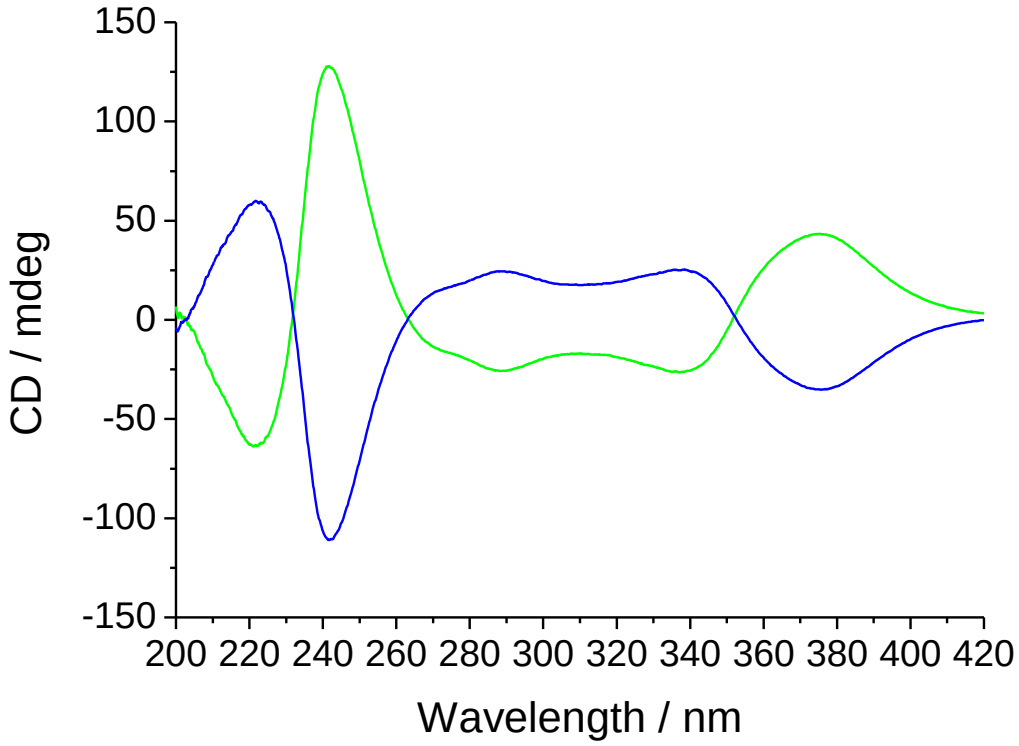

Figure S7. Circular dichroism spectra for ΔΔΔΔ -(K^+/*S*-nic^+)$_{11}$[$Ga_4L_6^{12-}$⊃ *S*-nic^+] (blue) and ΛΛΛΛ-(K^+/*S*-nic^+)$_{11}$[$Ga_4L_6^{12-}$⊃ *S*-nic^+] (green). Samples were recorded at a sample concentration of 0.05 mM, in the presence of 10 mM KOH in H_2O.

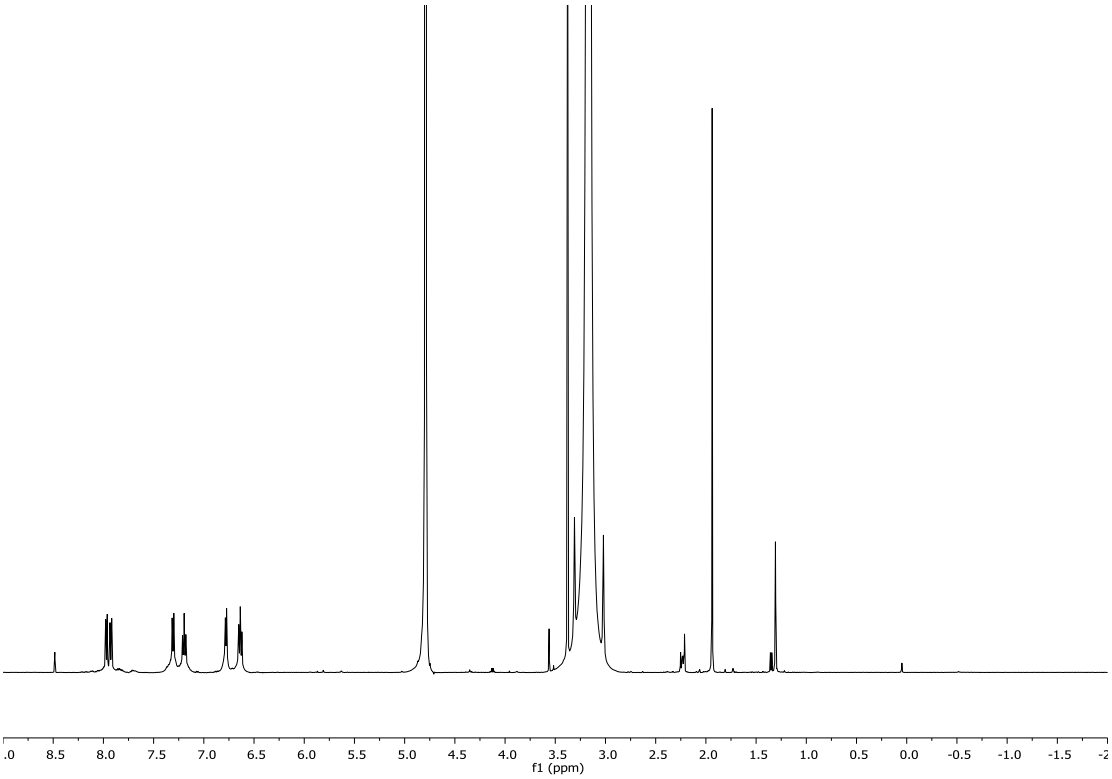

Figure S8. ^{1}H NMR (500 MHz, D_2O) of ΔΔΔΔ-$(NMe_4^+)_{11}[Ga_4L_6^{12-}\supset NMe_4^+]$ following ion-exchange chromatography.

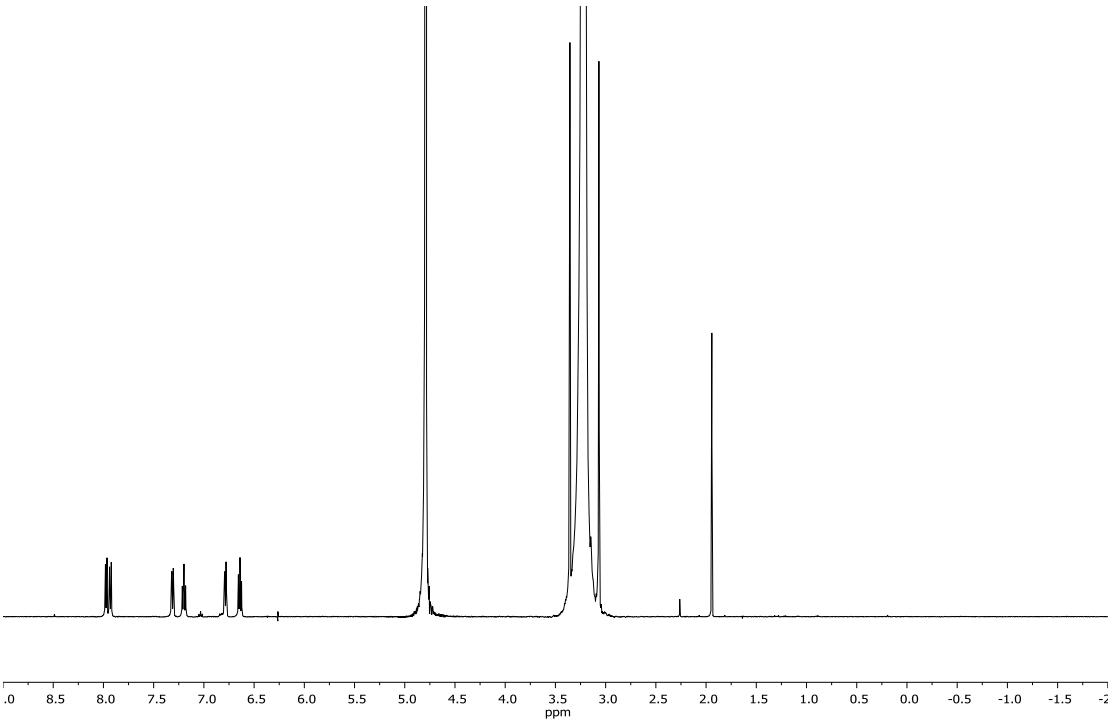

Figure S9. ^{1}H NMR (500 MHz, D_2O) of ΛΛΛΛ-$(NMe_4^+)_{11}[Ga_4L_6^{12-}\supset Me_4N^+]$ following ion-exchange chromatography.

2. Single-channel recordings

Single channel experiments were performed at room temperature (21 ± 2 ˚C) in a custom built cell, composed of two *Teflon* blocks each with a machine-drilled well ~1 mL in volume that were bolted together. Each well contained a side opening such that when the blocks are clamped together the wells are connected through their side openings. A 25 μm thick *Teflon* sheet (Goodfellow) was clamped between the two blocks, separating the side openings and fixed in place with silicone glue (3140 RTV coating, Dow Corning). A *Teflon* sheet containing an aperture of ~100 μm diameter (produced with a 30 kV spark gap generator) was positioned such that the aperture was in the centre of the lower half of the inter-well channel. The cell was placed on a Nano 20/30 anti-vibration platform (Halcyonics) within a custom built Faraday cage with acoustic damping to isolate the experiment from external electrical and mechanical noise. A small hanging drop (~5 μL) of 10% (*v*/*v*) solution of hexadecane in *n*-pentane was touched on each side of the *Teflon* sheet. 600 μL of a solution of KCl (1 M) and Tris–DCl (30 mM) buffered to pD 7.6 in D_2O was added to the well on each side of the *Teflon* sheet. 6 μL of 10 mg/mL solution of 1,2-diphytanoyl-*sn*-glycero-3-phosphocholine (Avanti Polar Lipids) in *n*-pentane was dispensed using a syringe on each side of the *Teflon* sheet. The buffer solution was then aspirated and dispensed into each well multiple times using a Hamilton syringe to paint a phospholipid bilayer across the aperture. Ag/AgCl electrodes (Warner) connected to a patch clamp amplifier (Axopatch 200B, Molecular Devices) were placed on either side of the *Teflon* sheet and a ±1 mV pulse applied at 1333 Hz to determine when a bilayer was obtained (capacitance of 50 to 80 pF). α-Hemolysin was introduced to the bilayer through one of two methods, as previously reported.[4]

2.1 Coordination cage experiments

Experiments with coordination cages were performed at room temperature (21 ± 2 ˚C). In a typical experiment, a single channel was acquired as described above and a potential of +100 mV was then applied across the lipid bilayer (live electrode in the well containing to *trans*-opening of the α-hemolysin). To the well containing the *cis*-opening of the pore was then added an aliquot of the coordination cage under investigation (typically 2.5–10 μL of a ~0.00625 mM solution, such that the final concentration of coordination cage was ~25–100 nM). All data were collected using the patch clamp amplifier (Axopatch 200B, Molecular Devices), and digitized using an Axon Instruments Digidata 1332A at a sampling rate of 50 kHz. Single-channel ion current recordings were processed unfiltered with Clampex 10.2 and Clampfit 10.2 software. Sample traces of individual experiments are shown below.

2.2 Single channel data

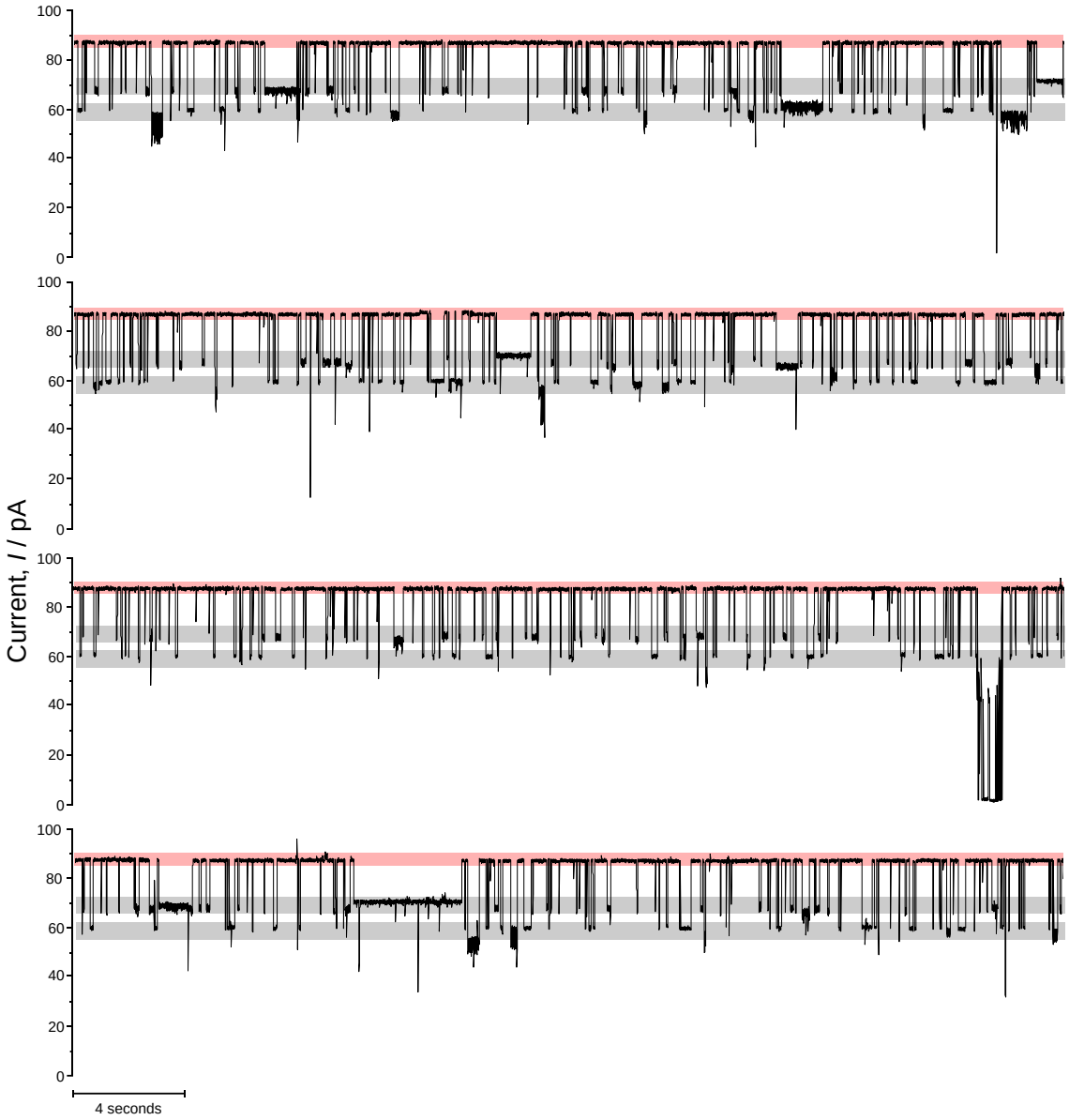

Figure S10. Extended ion-current trace from the addition of racemic $(K^+/NMe_4^+)_{11}[Ga_4L_6^{12-}\supset NMe_4^+]$ to the *cis*-side of a single α-hemolysin channel. Each well of the setup initially contained 600 µL of buffer containing 1 M KCl, 30 mM Tris-DCl at pD 7.6 in D_2O. To the ground well was added 7.5 µL of a solution of racemic $(K^+/NMe_4^+)_{11}[Ga_4L_6^{12-}\supset NMe_4^+]$ at a concentration of approximately 0.00625 mM, yielding a final concentration of coordination cage of approximately 75 nM. The experiment was conducted at a temperature of 21 ± 2 °C. Free pore current (marked in red) deviations could be divided into two levels (marked in gray), which corresponded to the two coordination cage enantiomers present in solution and comprised the majority of data-points recorded for analysis.

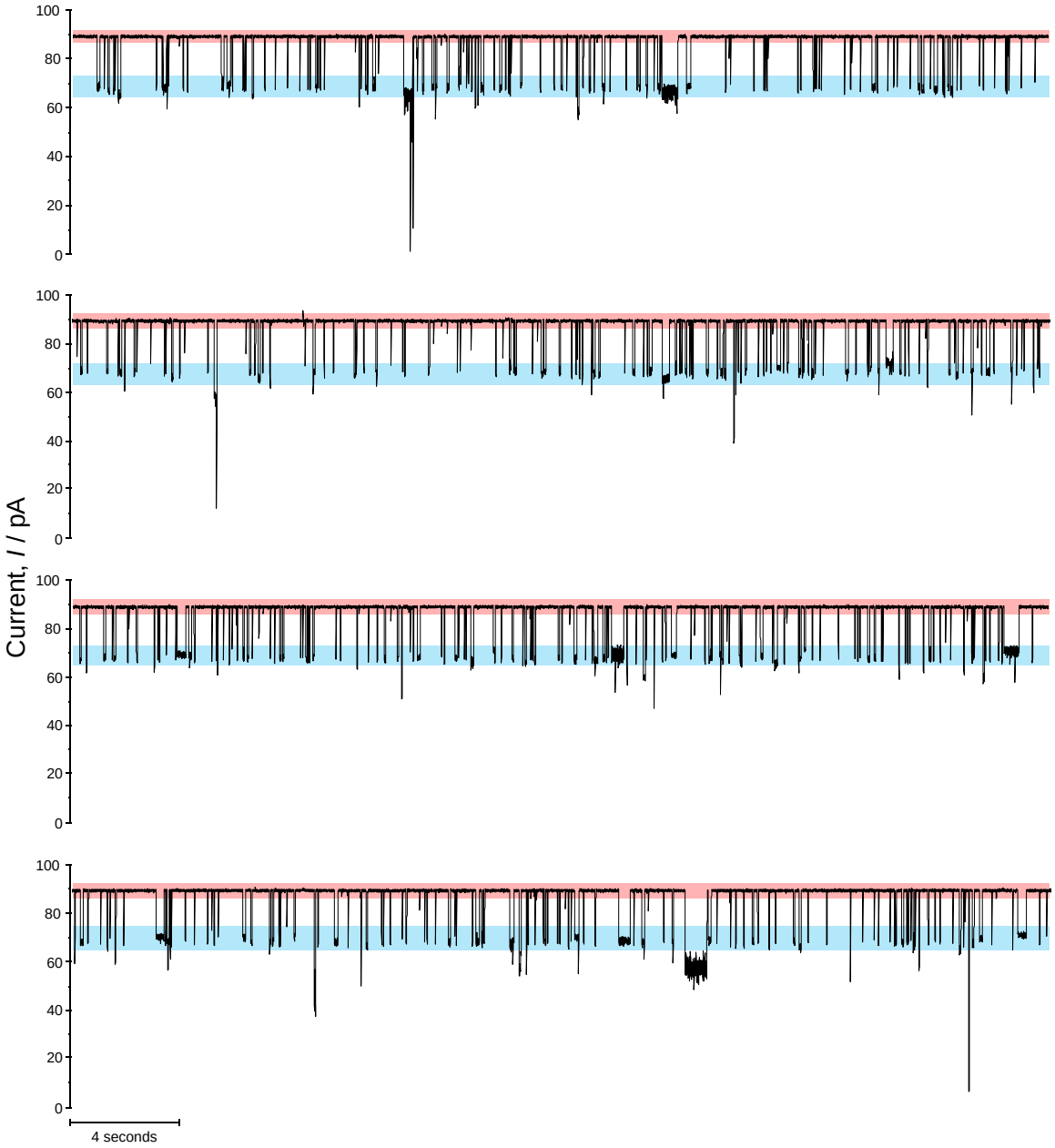

Figure S11. Extended ion-current trace from the addition of ΔΔΔΔ-$(NMe_4^+)_{11}[Ga_4L_6^{12-}\supset NMe_4^+]$ to the *cis*-side of a single α-hemolysin channel. Each well of the setup initially contained 600 µL of buffer containing 1 M KCl, 30 mM Tris-DCl at pD 7.6 in D_2O. To the ground well was added 7.5 µL of a solution of enantiomerically pure ΔΔΔΔ-$(NMe_4^+)_{11}[Ga_4L_6^{12-}\supset NMe_4^+]$ at a concentration of approximately 0.00625 mM, yielding a final concentration of coordination cage of approximately 75 nM. The experiment was conducted at a temperature of 21 ± 2 °C. Free pore current (marked in red) deviations generally went to a single level (marked in blue), which corresponded to the ΔΔΔΔ stereoisomer present in solution and comprised the majority of data-points recorded for analysis.

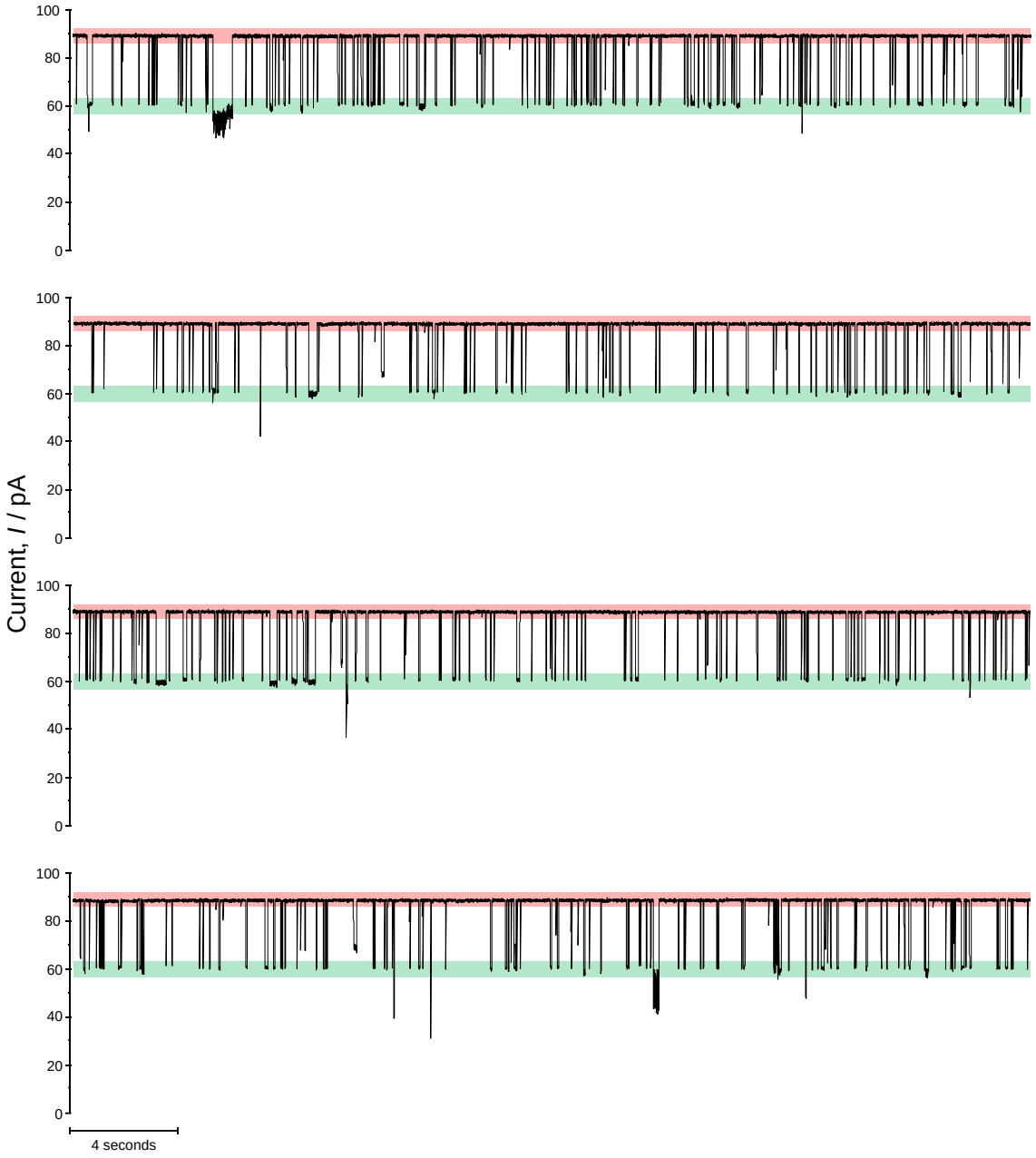

Figure S12. Extended ion-current trace from the addition of ΛΛΛΛ-$(NMe_4^+)_{11}[Ga_4L_6^{12-}\supset NMe_4^+]$ to the *cis* side of a single α-hemolysin channel. Each well of the setup initially contained 600 µL of buffer containing 1 M KCl, 30 mM Tris-DCl at pD 7.6 in D_2O. To the ground well was added 7.5 µL of a solution of enantiomerically pure ΛΛΛΛ-$(NMe_4^+)_{11}[Ga_4L_6^{12-}\supset NMe_4^+]$ at a concentration of approximately 0.00625 mM, yielding a final concentration of coordination cage of approximately 75 nM. The experiment was conducted at a temperature of 21 ± 2 °C. Free pore current (marked in red) deviations generally went to a single level (marked in green), which corresponded to the ΛΛΛΛ stereoisomer present in solution and comprised the majority of data-points recorded for analysis.

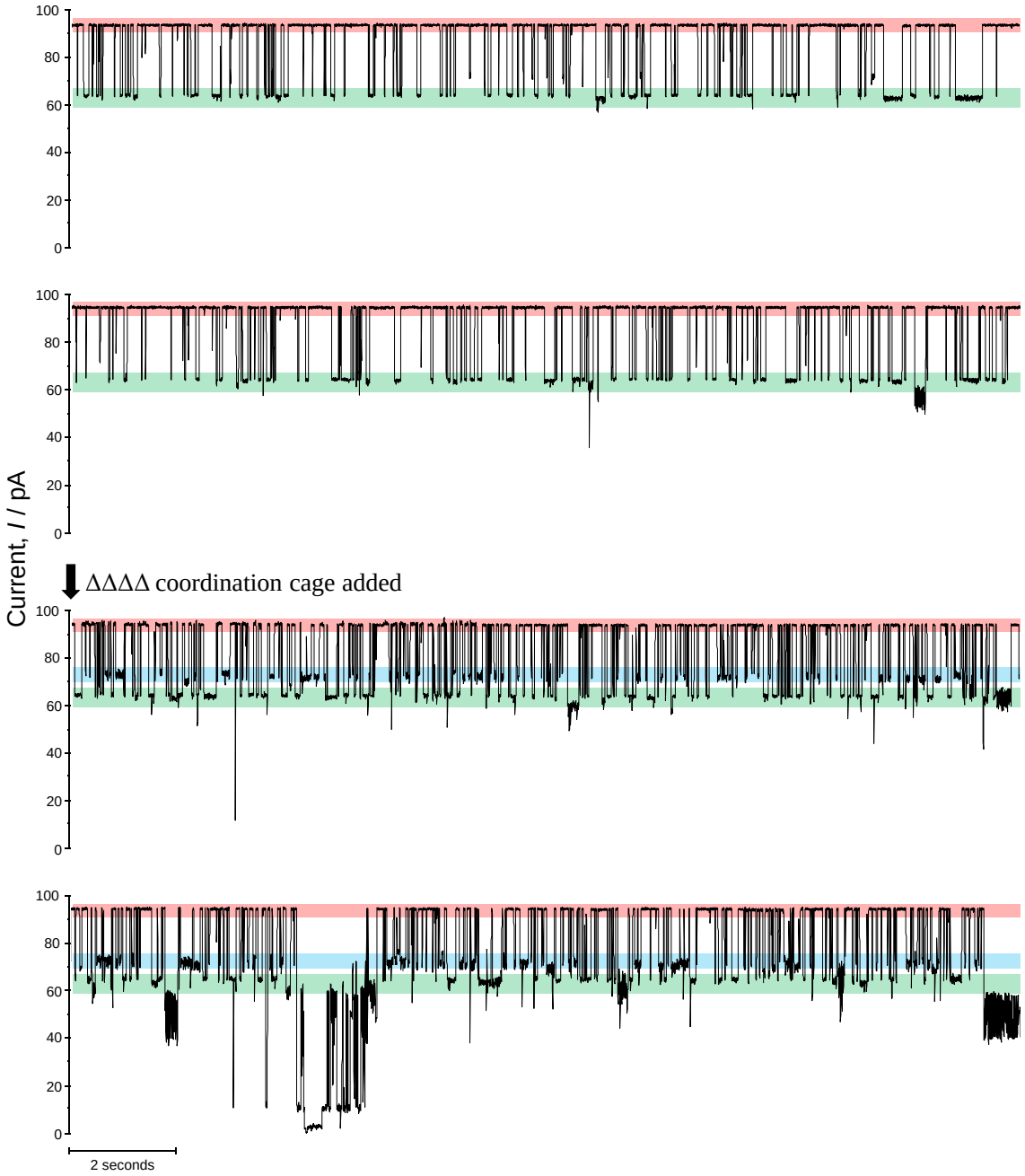

Figure S13. Extended ion-current trace from the addition of ΛΛΛΛ-$(NMe_4^+)_{11}[Ga_4L_6^{12-}\supset NMe_4^+]$, followed by ΔΔΔΔ-$(NMe_4^+)_{11}[Ga_4L_6^{12-}\supset NMe_4^+]$ to the cis side of a single α-hemolysin channel. Each well of the setup initially contained 600 µL of buffer containing 1 M KCl, 30 mM TRIS-DCl at pD 7.6 in D_2O. The experiment was conducted at a temperature of 21 ± 2 °C. To the ground well was added 15 µL of a solution of enantiomerically pure ΛΛΛΛ-$(NMe_4^+)_{11}[Ga_4L_6^{12-}\supset NMe_4^+]$ at a concentration of approximately 0.00625 mM, yielding a final concentration of coordination cage of approximately 150 nM (top two traces). Free pore current (marked in red) deviations generally went to a single level (marked in green). To the ground well was then added 15 µL of a solution of enantiomerically pure ΔΔΔΔ-$(NMe_4^+)_{11}[Ga_4L_6^{12-}\supset NMe_4^+]$ at a concentration of approximately 0.00625 mM. This resulted in a new current level being observed (marked in blue) which corresponded to the ΔΔΔΔ cage. The current levels observed were commensurate with those observed in earlier experiments (see Figure S12 and Figure S12).

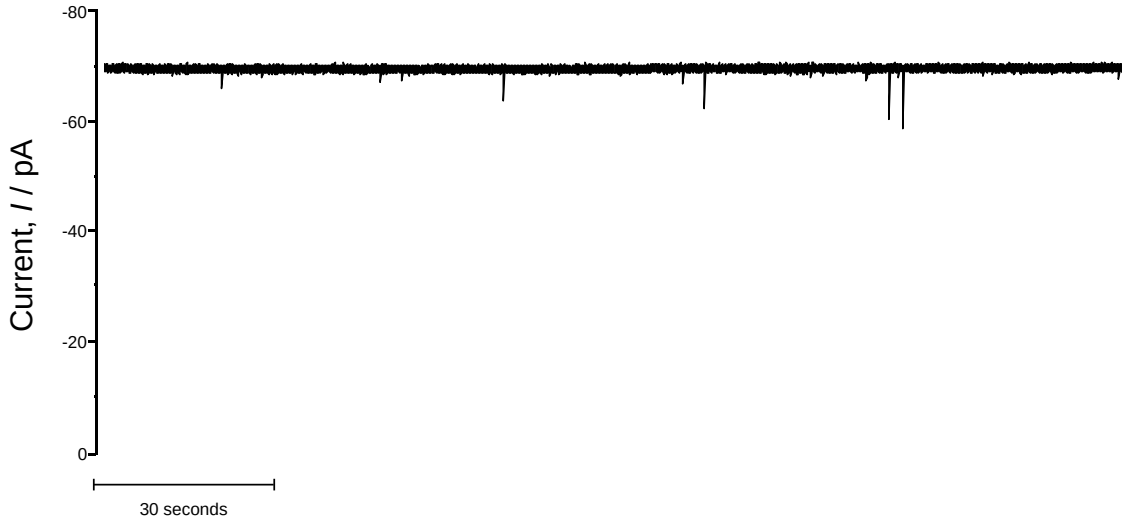

Figure S14. Sample ion current trace from the addition of racemic $(K^+/NMe_4^+)_{11}[Ga_4L_6^{12-}\supset NMe_4^+]$ to the *trans*-opening of a single α-hemolysin channel. Each well of the setup initially contained 600 µL of buffer containing 1 M KCl, 30 mM Tris-DCl at pD 7.6 in D_2O.

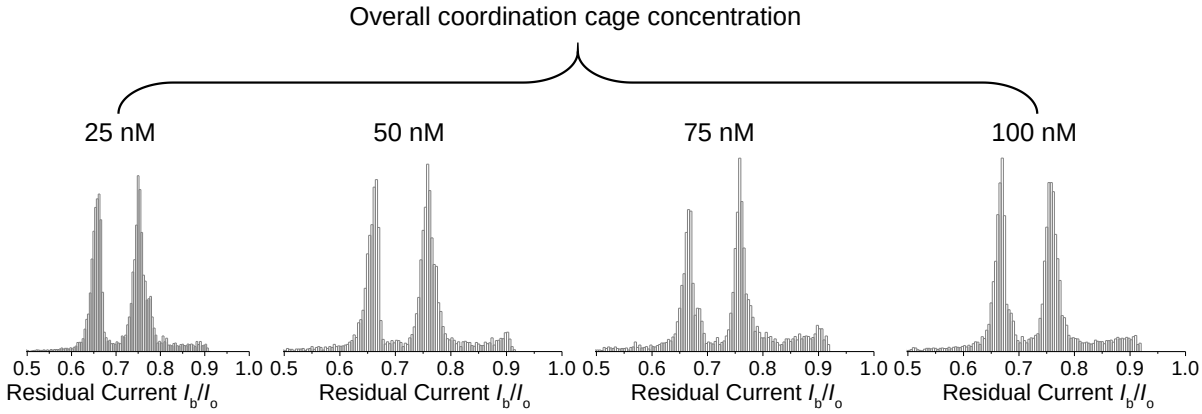

Figure S15. Histograms of racemic $(K^+/NMe_4^+)_{11}[Ga_4L_6^{12-}\supset NMe_4^+]$ over four concentrations, demonstrating that there is minimal change in the overall distribution of events across the two major current levels observed. This suggests that only one coordination cage occupies the nanopore at any one time.

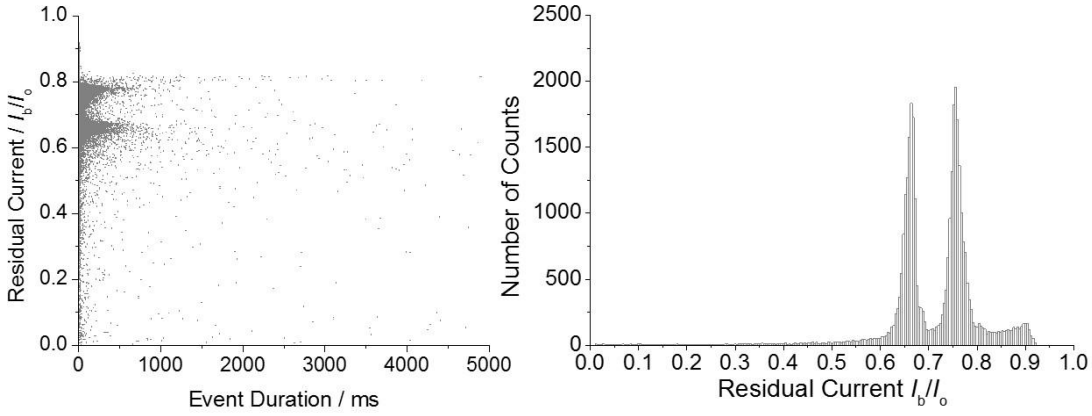

Figure S16. Scatter plot and frequency count histogram for racemic $(K^+/NMe_4^+)_{11}[Ga_4L_6^{11-}\supset Me_4N^+]$. Data is pooled from eleven pores and comprises 34,000 events. Histogram bin sizes are set at 0.004 I_b/I_o.

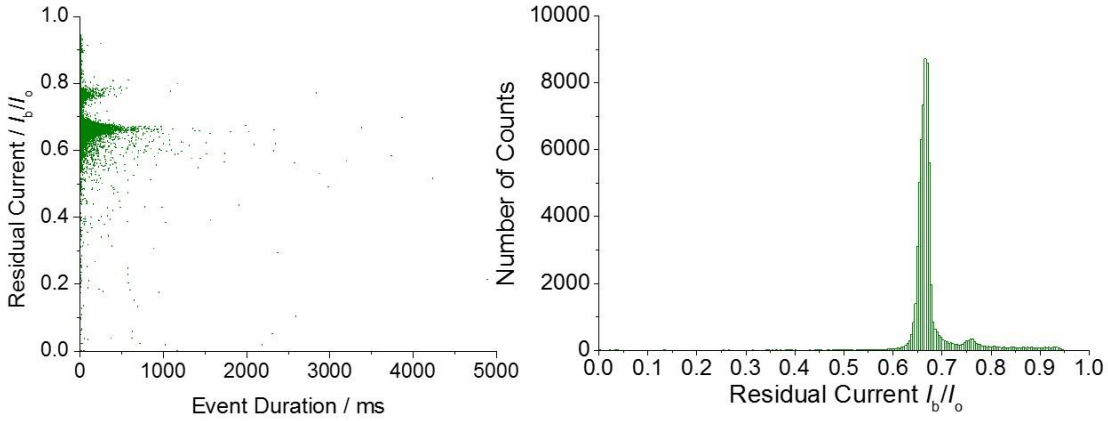

Figure S17. Scatter plot and frequency count histogram for ΛΛΛΛ-$(NMe_4^+)_{11}[Ga_4L_6^{11-}\supset Me_4N^+]$. Data is pooled from six pores and comprises 77,000 events. Histogram bin sizes are set at 0.004 I_b/I_o.

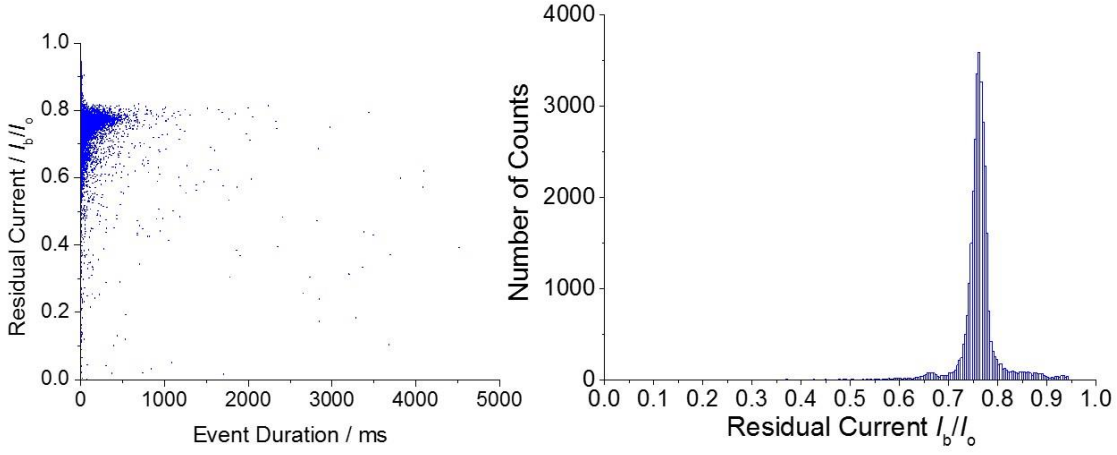

Figure S18. Scatter plot and frequency count histogram for ΔΔΔΔ-$(NMe_4^+)_{11}[Ga_4L_6^{11-}\supset Me_4N^+]$. Data is pooled from six pores and comprises 37,000 events. Histogram bin sizes are set at 0.004 I_b/I_o.

3. Kinetic analysis

Solutions of ΔΔΔΔ-$(NMe_4^+)_{11}[Ga_4L_6^{11-}\supset Me_4N^+]$ and ΛΛΛΛ-$(NMe_4^+)_{11}[Ga_4L_6^{11-}\supset Me_4N^+]$ were made up in D_2O and their concentrations determined through comparison with an ^{i}PrOH internal standard by ^{1}H NMR. The solutions of each chiral form were then diluted down to obtain stock solutions of both cages of 0.00625 mM. Aliquots of these solutions were then added to the 600 µL of buffer in the wells of patch clamp experiments, such that the concentration of cage in the experiment was one of 25, 50, 75 or 100 nM. Data was recorded for each enantiomer at final coordination cage concentrations of 25, 50, 75 and 100 nM as described in single channel recordings. The data was baseline corrected and filtered using at 200 Hz using the *Lowpass Bessel* (8-pole) filter in Clampfit 10.4 and events detected using the *Threshold Search* method in Clampfit 10.4. Events that did not correspond to the chiral form under investigation were discarded from the final datasets used for kinetic analysis (see Figure S19).

As not all events that occur during patch clamp experiments are due to coordination cages interacting with the nanopore, the data was manually filtered according to the thresholds indicated on the histograms in Figure S19 and the events not corresponding to coordination cages were excluded from the analysis. The mean duration of events (τ_{off}) and mean inter-event durations (τ_{on}) of each chiral form of at concentrations of 25, 50, 75 and 100 nM were determined by plotting frequency count histograms of the collated data from all pores at (bin sizes = 8 ms). The histograms were then fitted to single exponential decay curves in Origin 8.5.1 and half-lives obtained which corresponded to τ_{off} and τ_{on}. Error bars for data points at each concentration were obtained by taking the standard deviation of τ_{off} and τ_{on} values obtained for individual pores at each concentration (25, 50, 75 and 100 nM).

Assuming bimolecular kinetics are in operation (inferred from the exponential fit of histograms), the rate constants for association (k_{on}) and dissociation (k_{off}) can be calculated as follows: $k_{on} = 1/\tau_{on} \cdot c$ (where c is the concentration of the coordination cage in solution) and $k_{off} = 1/\tau_{off}$. A value of k_{on} for each chiral form of coordination cage was obtained from the slope of the graph $1/\tau_{on}$ vs cage concentration (see Figure 3 main text). A value for k_{off} for each chiral form of coordination cage was obtained from the intercept value (mean τ_{off} for each cage across all experiments) obtained from the graph of $1/\tau_{off}$ vs cage concentration (see Figure 3 main text). Errors for k_{on} and k_{off} were estimated from linear regression analyses of the data used to plot $1/\tau_{on}$ vs cage concentration and $1/\tau_{off}$ vs cage concentration graphs respectively. Equilibrium association constants (K_a) for each chiral form with α-HL were obtained from the relationship $K_a = k_{on} / k_{off}$ and errors in K_a values were estimated using the root mean square method.

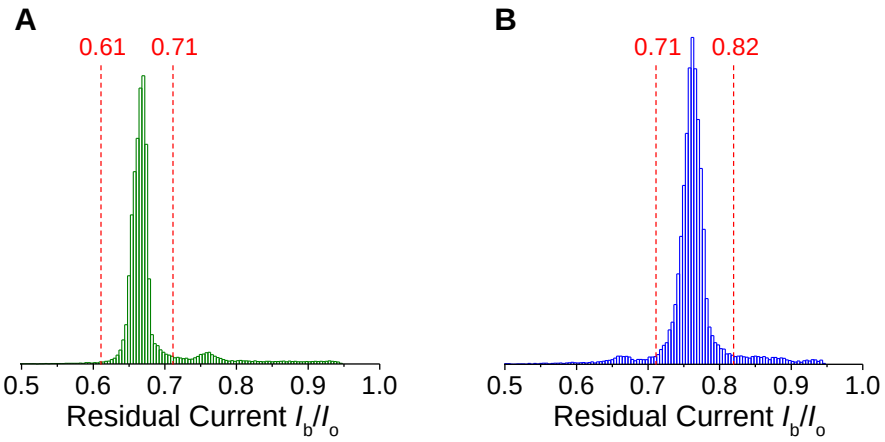

Figure S19. Illustration of the manual filters applied to exclude events that did not correspond to specific enantiomers of cage for (**A**) ΛΛΛΛ-$(NMe_4^+)_{11}[Ga_4L_6^{12-}\supset Me_4N^+]$ and (**B**) ΔΔΔΔ-$(NMe_4^+)_{11}[Ga_4L_6^{12-}\supset Me_4N^+]$.

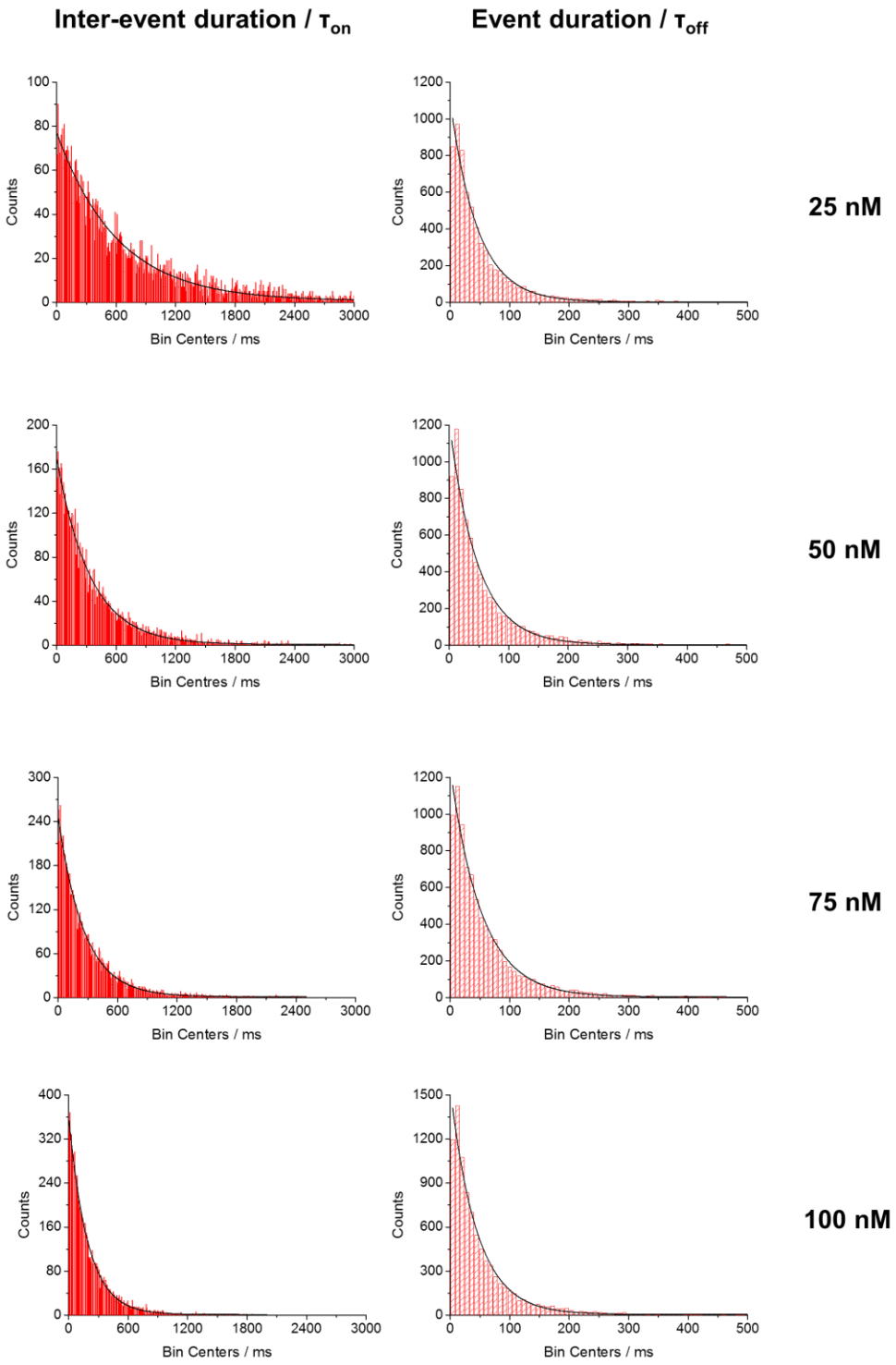

Figure S20. Event duration (τ_{off}) and inter-event duration (τ_{on}) histograms and fitted exponential decay curves for kinetic analysis of the interaction between ΔΔΔΔ-$(NMe_4^+)_{11}[Ga_4L_6^{12-}\supset NMe_4^+]$ and α-HL. Data at each concentration obtained from at least three separate nanopore experiments.

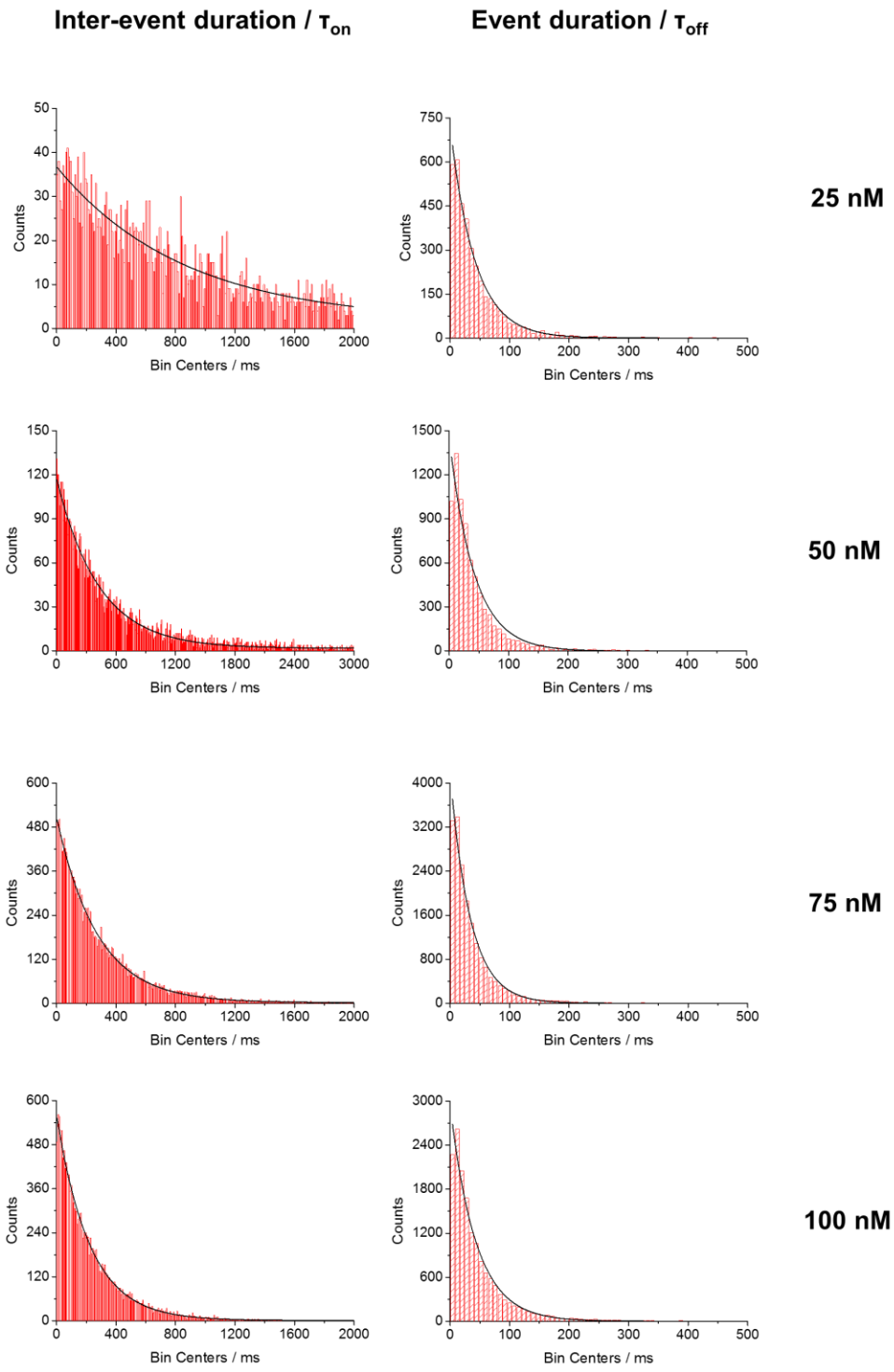

Figure S21. Event duration (τ_{off}) and inter-event duration (τ_{on}) histograms and fitted exponential decay curves for kinetic analysis of the interaction between ΛΛΛΛ-$(NMe_4^+)_{11}[Ga_4L_6^{12-}\supset NMe_4^+]$ and α-HL. Data at each concentration obtained from at least three separate nanopore experiments.

4. Method for calculating enantiomer concentrations in mixed solutions

Solutions of the ΛΛΛΛ (0.260 mM) and ΔΔΔΔ (0.839 mM) chiral forms (as Me_4N^+ salts) were combined in known quantities and made up to a total volume of 100 µL such that the molar ratio of ΛΛΛΛ / ΔΔΔΔ was 70:30 (16.8 µL of ΛΛΛΛ and 2.2 µL of ΔΔΔΔ, 81 µL of buffer) and 30:70 (7.2 µL of ΛΛΛΛ and 5.2 µL of ΔΔΔΔ, 87.6 µL of buffer). 7.5 µL of the mixture under investigation was then added to an experiment set up (total concentration of cage in experimental setup is 75 nM) and data recorded as detailed in 'single channel recordings'. The number of counts for each chiral form were obtained by filtering events (event currents normalised to the free pore current) in each experiment such that only the events corresponding to each chiral form remained.

We hypothesized that the kinetic data obtained for the individual chiral forms from experiments with enantiopure samples should allow the concentrations of coordination cages in an enantio-enriched sample to be determined. The inter-event duration (τ_{on}) for a chiral form over a given period of time should be inversely proportional to the number of counts of observed (i.e. a high number of counts will give rise to a low value for τ_{on}). In the case of a 'mixed' sample of ΛΛΛΛ / ΔΔΔΔ enantiomers, we can therefore state the following:

$$\frac{T_{on_\Delta}}{T_{on_\Lambda}} = \frac{\Lambda_{count}}{\Delta_{count}}$$

Using the relationship $k_{on} = 1/\ \tau_{on} \cdot c$ described earlier, we can describe this relationship in terms of concentrations and dissociation constants:

$$\frac{k_{on_\Lambda}[\Lambda]}{k_{on_\Delta}[\Delta]} = \frac{\Lambda_{count}}{\Delta_{count}}$$

We can rearrange to solve for the concentration of one chiral form alone (in this case the ΛΛΛΛ form – represented here as [Λ]):

$$[\Lambda] = \frac{\Lambda_{count} k_{on_\Delta}[\Delta]}{\Delta_{count} k_{on_\Lambda}}$$

Given that:

$$[cage]_{total} = [\Delta] + [\Lambda] \rightarrow \qquad [\Delta] = [cage]_{total} - [\Lambda]$$

We can then state:

$$[\Lambda] = \frac{\Lambda_{count} k_{on_\Delta}([cage]_{total} - [\Lambda])}{\Delta_{count} k_{on_\Lambda}}$$

Thus we can rearrange to solve for [Λ] using the known ($k_{on\Lambda}$ and $k_{on\Delta}$) and observed (Λ_{count} and Δ_{count}) terms:

$$\Delta_{count} k_{on_\Lambda}[\Lambda] = \Lambda_{count} k_{on_\Delta}[cage]_{total} - \Lambda_{count} k_{on_\Delta}[\Lambda]$$

$$\Delta_{count} k_{on_\Lambda}[\Lambda] + \Lambda_{count} k_{on_\Delta}[\Lambda] = \Lambda_{count} k_{on_\Delta}[cage]_{total}$$

$$[\Lambda]\left(\Delta_{count} k_{on_\Lambda} + \Lambda_{count} k_{on_\Delta}\right) = \Lambda_{count} k_{on_\Delta}[cage]_{total}$$

$$[\Lambda] = \frac{\Lambda_{count} k_{on_\Delta}[cage]_{total}}{\Delta_{count} k_{on_\Lambda} + \Lambda_{count} k_{on_\Delta}}$$

$$[\Lambda] = \frac{\Lambda_{count} k_{on_\Delta}}{\Delta_{count} k_{on_\Lambda} + \Lambda_{count} k_{on_\Delta}} \cdot [cage]_{total}$$

To solve for [Δ], terms relating to the ΛΛΛΛ / ΔΔΔΔ forms are simply reversed. The calculated and observed values for [Λ] and [Δ] are shown in Table S1.

	Total cage concentration ~75 nM[a]				**Total cage concentration ~100 nM[a]**			
ΛΛΛΛ / ΔΔΔΔ mol/mol	**$[\Lambda]_{calc}$[b] / nM**	**$[\Lambda]_{obs}$[c] / nM**	**$[\Delta]_{calc}$[b] / nM**	**$[\Delta]_{obs}$[c] / nM**	**$[\Lambda]_{calc}$[b] / nM**	**$[\Lambda]_{obs}$[c] / nM**	**$[\Lambda]_{calc}$[b] / nM**	**$[\Delta]_{obs}$[c] / nM**
70:30	53.9±5.4	54.9±5.8	22.8±2.3	21.8±2.3	71.6±7.2	72.2±7.6	30.3±3.0	29.7±3.1
30:70	23.1±2.3	28.3±3.3	53.9±5.4	48.6±5.7	30.7±3.1	37.2±4.4	71.5±7.2	65.0±6.9

Table S1. Observed and calculated concentrations of individual ΛΛΛΛ and ΔΔΔΔ enantiomers in pre-determined mixtures thereof, as indicated in the first column.[a] Actual total cage concentrations were: a) 70:30 ΛΛΛΛ / ΔΔΔΔ: 76.7 nM and 101.9 nM; b) 30:70 ΛΛΛΛ / ΔΔΔΔ: 76.9 nM and 102.2 nM.[b] Errors in calculated concentrations of enantiomeric forms were conservatively estimated at 10%.[c] Errors in observed concentrations of enantiomers were estimated to be 10.6% for ΔΔΔΔ and 11.8% for ΛΛΛΛ and were determined using a root squares method.

Supporting references

(1) Seeman, J. I.; Whidby, J. F. *J. Org. Chem.* **1976**, *41*, 3824.
(2) Davis, A. V.; Fiedler, D.; Ziegler, M.; Terpin, A.; Raymond, K. N. *J. Am. Chem. Soc.* **2007**, *129*, 15354.
(3) Caulder, D. L.; Powers, R. E.; Parac, T. N.; Raymond, K. N. *Angew. Chem. Int. Ed.* **1998**, *37*, 1840.
(4) Holden, M. A.; Bayley, H. *J. Am. Chem. Soc.* **2005**, *127*, 6502.